Analytical Biochemistry 587 (2019) 113432

Contents lists available at ScienceDirect

Analytical Biochemistry

journal homepage: www.elsevier.com/locate/yabio

Visual detection of kanamycin with DNA-functionalized gold nanoparticles probe in aptamer-based strip biosensor

Ying Ou, Xin Jin, Jing Liu, Yaping Tian, Nandi Zhou*

The Key Laboratory of Carbohydrate Chemistry and Biotechnology, Ministry of Education, School of Biotechnology, Jiangnan University, Wuxi, 214122, China

ARTICLE INFO

Keywords:
Lateral flow strip biosensor
Kanamycin
Aptamer
Gold nanoparticles
Magnetic microspheres

ABSTRACT

Kanamycin has been widely used to treat human and animal diseases. The excessive use of kanamycin causes its accumulation in animal-derived foods, and eventually threats human health. In the present study, we develop a lateral flow strip biosensor for fast and sensitive detection of kanamycin. The strip biosensor combines the easy separation of magnetic microspheres (MMS) with target-mediated chain displacement of single-stranded DNA and the capture of the visible DNA-functionalized gold nanoparticles (AuNPs) probe. The presence of kanamycin can competitively bind to the aptamer and release cDNA to the supernatant. The concentration of free cDNA, which is the direct target of the strip, is proportional to the concentration of kanamycin. The capture of DNA-functionalized AuNPs on the test zone of the strip through cDNA-induced hybridization provides a visual detection signal. The assay can be completed within 20 min. The visual detection limit by naked eyes of the strip is 50 nM. A linear detection range of 5–500 nM is derived for quantitative determination, with the detection limit of 4.96 nM (S/N = 3). This lateral flow strip biosensor can quickly and sensitively detect kanamycin in different food samples, which holds great application potential in medicine and daily life.

1. Introduction

Antibiotics are secondary metabolites produced by bacteria, fungi, animals or plants, which have diverse anti-pathogens activities. Among them, aminoglycoside antibiotics have been widely used due to their advantages over other categories of antibiotics, such as low cost, good water solubility, broad antibacterial spectrum and good therapeutic effect against common bacterial diseases [1]. Kanamycin, one of the most frequently used aminoglycoside antibiotics, is produced by fermentation of *Streptomyces kanamyceticus* [2]. Kanamycin can lead to the misreading of the genetic code and bind to 30S subunit of ribosome to inhibit translation, thereby inhibit the growth and reproduction of Gram-negative and Gram-positive bacteria [3,4]. With the increasing use, especially overcommitment of kanamycin, its residue in animal-derived food, water and human body threats our health due to its ototoxicity, nephrotoxicity and neurotoxicity [5,6]. Recently, it has become a serious public health issue on a global scale [7]. The European Commission has set maximum residue limits (MRLs) for kanamycin at 150 μg/kg in milk [8,9]. In order to secure the quality and safety of food, it is necessary to develop simple and rapid assays for kanamycin. A variety of detection methods for kanamycin residues have been reported, such as high performance liquid chromatography (HPLC) [10], capillary zone electrophoresis (CZE) [11], surface plasmon resonance (SPR) [12], enzyme-linked immunosorbent assay (ELISA) [13], and electrochemical detection [14,15]. However, the environment and market administration requires convenient, fast, economical, accurate and sensitive assays which can be applied in on-site visual mode [16,17].

Since there is an increasing demand for surveillance of infectious diseases and food hygiene, particularly in underdeveloped areas, the development of rapid assay kits has attracted research interest. The lateral flow strips are able to test and diagnose at any location outside the laboratory [18] and have been widely used in human testing, veterinary diagnostics, industrial, food and environmental testing [19,20]. Up to now, strip biosensors have also been developed for antibiotics detection. These strips generally use antibodies as recognition elements. However, the types and application of these strips are severely limited, mainly restricted by the cost and availability of the antibiotics-specific recognition elements. Aptamers are functional nucleic acids, typically short-chain single-stranded DNAs or RNAs. When aptamers bind to targets, their conformation will change to form hairpin, conve xring, stem ring, G-quadruplex or other special structures to accommodate the targets specifically [21]. Aptamers can recognize and bind to a very broad range of targets, including small molecules, biological macromolecules, organisms, *etc*. Thus, aptamers can serve as a tool with great potential for analysis, diagnosis and

* Corresponding author.
E-mail address: zhounandi@jiangnan.edu.cn (N. Zhou).

https://doi.org/10.1016/j.ab.2019.113432
Received 22 July 2019; Received in revised form 10 September 2019; Accepted 12 September 2019
Available online 12 September 2019
0003-2697/

treatment. Meanwhile, the preperties of aptamers are even superior to antibodies in high specificity, high stability, ease of modification and regeneration [22,23]. Recently, the test strips technology based on aptamers has been greatly developed and applied [24]. Even though, aptamer-based lateral flow strip biosensors for antibiotics have seldom been reported, which may be ascribed to the availability of effective aptamers for antibiotics. As potential products for scalable application, the configuration and performance of strip biosensors need to be robust. In the mean time, the requirements for the aptamers to competitively bind to the targets or hybridize with complementary sequences on the strips are usually more stringent than those in solution. The stability of the affinity of aptamers in different environment, as well as the appropriate binding strength to the targets and complementary sequences are the major factors which define the performance of the strip biosenors. The report of the aptamers for antibiotics with high specificiety, high affinity and appropriate length of the sequence, such as aptamers for kanamycin [25] and tobramycin [26,27], offers the opportunity for the fabrication of aptamer-based strip biosensors for antibiotics.

We previously developed an aptamer and functionalized nanoparticle-based dry-reagent strip biosensor for kanamycin [28]. Although the analytical performance of the strip biosensor is satisfactory, the T zone exhibiting lighter or faded band (negative result) in the presence of kanamycin is not in accordance with the regular way. Moreover, the occurrence of a new band on the T zone in the presence of the target is generally more sensitive for visual observation than that of the gradually faded band. In this study, we develop another aptamer-based strip biosensor for kanamycin with different configuration. In this strip biosensor, DNA1-functionalized gold nanoparticles (AuNPs-DNA1) are used as the color indicating probe, and magnetic microspheres (MMS) are used to fast separation of cDNA, which is the secondary target of the assay produced by kanamycin. Thus qualitative and semi-quantitative detection of kanamycin can be achieved by naked eyes and a scanning reader, respectively.

2. Materials and methods

2.1. Materials and reagents

Streptavidin-modified magnetic microspheres (2 μm) were purchased from BaseLine ChromTech Research Centre (Tianjin, China). Kanamycin, tris-(2-carboxyethyl)-phosphine hydrochloride (TCEP), dATP and streptavidin were procured from Sangon Biotech Co., Ltd (Shanghai, China). Hydrogen tetrachloroaurate hydrate ($HAuCl_4{\cdot}3H_2O$) and sodium citrate were obtained from Sinopharm Chemical Reagent Co., Ltd (Shanghai, China). Nitrocellulose membrane, sample pad, conjugate pad, absorption pad and adhesive backing were from Jieyi Biotechnology Co., Ltd (Shanghai, China). Other chemicals were of analytical grade. All solutions were prepared with ultrapure water (18.2 MΩ cm) obtained from a Millipore water purification system.

All the oligonucleotides including kanamycin-specific aptamer, cDNA, DNA1, capDNA1 and capDNA2 were synthetized and HPLC-purified by Sangon Biotech Co., Ltd. These sequences are listed as follows:

Aptamer: 5′-Biotin-TGGGGGTTGAGGC*TAAGCCGA*-3’ [25].

cDNA: 5′-TTGTGCTA*TCGGCTTAC*-3’

DNA1: 5′-**ATAGCACAACC**GTC–$(CH_2)_6$–HS-3’

capDNA1: 5′- Biotin-TGACTGTAAGCCG-3’

capDNA2: 5′-**GGTTGTGCTAT**TATGA-Biotin-3’

Underlined, bold and italic letters represent the complementary sequences.

2.2. Synthesis and functionalization of gold nanoparticles

AuNPs were prepared according to previously reported procedures [29]. Briefly, 100 mL of 0.01% (w/v) $HAuCl_4$ was added into a 250 mL round bottom flask. Then the solution was stirred with heating. After boiling for 2 min, 3.5 mL of 1% (w/v) sodium citrate was quickly added with stirring. The mixture was stirred for 15 min at 100 °C, and then 30 min at room temperature. The prepared AuNPs were concentrated by heating until the final volume was 20 mL, and stored at 4 °C in the dark until use.

To prepare the functionalized AuNPs, the oligonucleotide DNA1 was covalently attached to the surface of AuNPs *via* Au–S bond. DNA1-functionalized AuNPs (AuNPs-DNA1) were prepared according to the previously reported procedure [30]. In brief, 15 μL of 1 mM TCEP and 30 μL of 100 μM DNA 1 were mixed to activate the thiol group of DNA1. Then 1 mL the above prepared AuNPs were added and the mixture was stirred at room temperature for 1 h. Subsequently, 30 μL of 15 mM dATP was added to the solution, and 35 min additional incubation was carried out with stirring. After that, 20 μL of 1 M NaCl was added, and incubated at room temperature for 30 min and at 4 °C for 6 h respectively, to improve the stability of the obtained nanoparticles. Finally, the mixture was centrifugated at 8000 rpm for 20 min at 4 °C to remove unbound DNA1. The supernatant was discarded and the pellet was re-suspended in 1 mL of 20 mM Na_3PO_4 solution (containing 5% BSA, 10% sucrose, 0.5% Tween-20 and 0.5% Triton X-100). The obtained AuNPs-DNA1 were stored at 4 °C in the dark.

2.3. Modification of magnetic microspheres

The particle size of the magnetic microspheres used in the experiment was 2 μm and the surface was modified with streptavidin. Firstly, 50 μL of cDNA (1 μM) and 50 μL of aptamer (1 μM) were placed at 95 °C for 3 min. Then they were incubated at 37 °C for 1 h to allow complete formation of apt-cDNA duplex between the complementary sequences of cDNA and aptamer. Since the surface of magnetic microspheres is modified with streptavidin and the aptamer is modified with biotin at 5′-end, apt-cDNA duplex can be coupled to the surface of magnetic microspheres *via* biotin-streptavidin interaction. The magnetic microspheres were washed 5 times with 10 mM PBS (pH 7.4). Then magnetic microspheres and apt-cDNA were shaken at 37 °C for 1 h to form MMS-apt-cDNA. The duplex-combined magnetic microspheres were washed three times with 10 mM PBS to remove unbound DNA. The prepared MMS-apt-cDNA were stored at 4 °C.

2.4. Preparation of streptavidin-biotin-capDNA1 and streptavidin-biotin-capDNA2 conjugates

CapDNA1 was designed to capture cDNA and further AuNPs-DNA1 on the test zone (T zone), whereas capDNA2 was designed to capture AuNPs-DNA1 on the control zone (C zone). The streptavidin-biotin-capDNAs (Str-Bio-capDNAs) conjugates were prepared using high affinity between streptavidin and biotin modified at the ends of capDNA1/capDNA2. 1 mg/mL streptavidin was prepared in 10 mM PBS (pH 7.4). Then 20 μL of 10 μM biotinylated capDNAs were respectively mixed with 5 μL streptavidin and incubated at 4 °C for 2 h to complete the binding between streptavidin and biotinylated capDNA1 and capDNA2. To block the remaining binding sites of streptavidin, the prepared Str-Bio-capDNA1/capDNA2 conjugates were incubated with 10 μL of 5 mM biotin. In order to remove excess DNA and biotin, centrifugation was carried out by using an ultrafiltration tube (MWCO 30 kDa). The prepared Str-Bio-capDNA1 and Str-Bio-capDNA2 were stored at 4 °C.

2.5. Assembly of the lateral flow strip biosensor

The strip biosensor consists of a sample pad (SP), a conjugate pad (CP), nitrocellulose membrane (NC membrane), an absorption pad (AP) and PVC adhesive backing (AB).

SP and CP were firstly cut into the appropriate size, and then immersed into the treatment solution (0.1 M Tris-HCl buffer containing 2% sucrose, 1% NaCl, 1% BSA, 1% TritonX-100 and 0.5% Tween-20, pH 8.2) for 30 min, fianlly dried at 45 °C. 20 μL of 4 μM AuNPs-DNA1

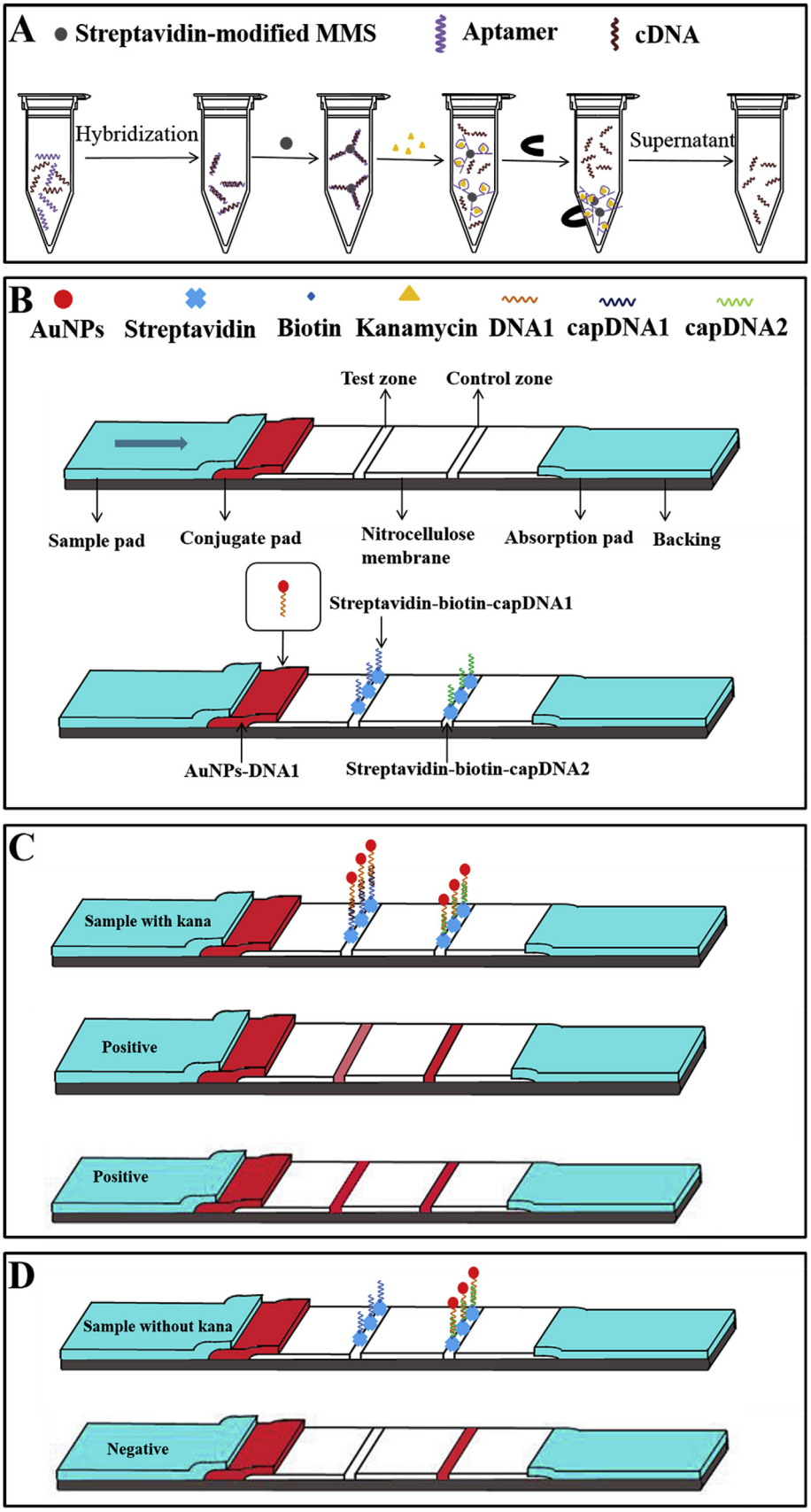

Scheme 1. Schematic diagram of configuration and detectiion principle of the strip biosensor. (A) Step 1: Sample pretreatment with MMS-apt-cDNA; (B) Step 2: The configuration of the strip biosensor; (C) Schematic diagram of the positive result in the presence of kanamycin; (D) Schematic diagram of the negative result in the absence of kanamycin.

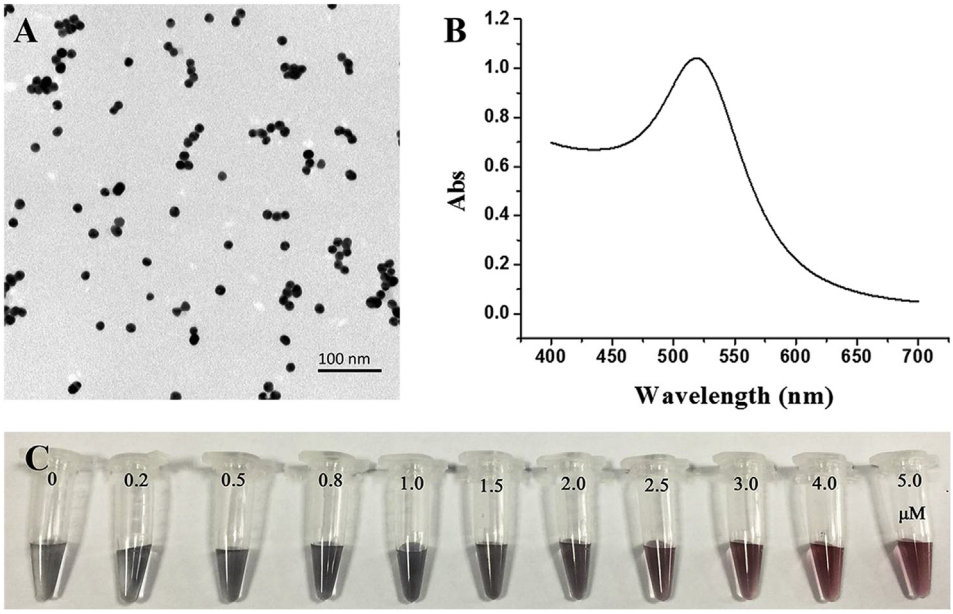

Fig. 1. (A) TEM image of AuNPs; (B) Absorption spectrum of AuNPs; (C) Color changes after incubation of AuNPs functionalized with different concentration of DNA1 in NaCl. (For interpretation of the references to color in this figure legend, the reader is referred to the Web version of this article.)

were spread evenly on CP, followed by drying at 37 °C for 2 h.

To prepare the lateral flow strip biosensor, the pads and NC membrane were firstly overlapped and pasted on AB (Scheme 1B). Then 1 μL Str-Bio-capDNA1 and Str-Bio-capDNA2 conjugates were respectively used to draw two lines on NC membrane near CP and AP to construct T zone and C zone. The distance between T zone and C zone was fixed as 5 mm. The assembled strips were dried at 37 °C for 1 h and stored in tin foil bags at 4 °C.

2.6. Detection of kanamycin

In this study, the concentration of kanamycin in samples is converted to the concentration of kanamycin-displaced cDNA from magnetic microspheres. And fast separation can also be achieved utilizing magnetic microspheres. The previously obtained MMS-apt-cDNA were washed three times and resuspended in the binding buffer (10 mM Tris-HCl containing 1 M NaCl, 1 mM EDTA and 0.05% Tween-20, pH 7.5). Then, 50 μL of kanamycin samples with different concentrations were added to the buffer. The mixture was kept for 10 min with shaking to allow kanamycin to bind to the aptamer, displace cDNA from the duplex and release cDNA from the magnetic microspheres to the solution. Upon the action of magnetic force, the magnetic microspheres were precipitated, and the supernatant was taken as the test solution.

The strips were placed in the cartridges before detection. Then 100 μL test solution was added into the sample well located on SP. The strips were then stood for 10 min to allow the migration of the test solution from SP to AP. Due to the accumulation of AuNPs on the T zone and C zone, two red bandscan be visually observed. The optical density of the T zone (expressed as the peak area) was measured using a scanning reader (Jieyi Biotechnology Co., Ltd, Shanghai, China) to quantitatively analyze the concentration of kanamycin.

For real sample detection, kanamycin was spiked into milk, honey and milk powder to prepare artificially kanamycin-contaminated samples. Pretreatment of the samples are required. For milk samples, 20% trichloroacetic acid was added dropwise to adjusted pH to 4.6. The samples were incubated at 45 °C for 10 min, followed by centrifugation at 10,000 r/min for 25 min to remove coagulated proteins and fat. For milk powder samples, after dissolving, the fat layer was removed by centrifugation at 10,000 r/min for 20 min. And the supernatant was diluted 10 folds with binding buffer. For honey samples, they were diluted 10 folds with binding buffer directly. Then the detection was carried out as described above.

3. Results and discussion

3.1. The configuration and detection principle of the strip

In this study, a DNA-functionalized AuNPs and aptamer-based strip biosensor for kanamycin is developed (Scheme 1). The assay can be divided into two steps. In step one, sample solution is pretreated with magnetic microspheres to convert the concentration of kanamycin in sample to the concentration of the released cDNA. The apt-cDNA duplex is firstly formed and combined to magnetic microspheres *via* the binding of biotin-streptavidin. When kanamycin sample is incubated with the prepared MMS-apt-cDNA, kanamycin binds specifically to the aptamer and releases cDNA from the duplex (Scheme 1A). The released cDNA is positively correlated with kanamycin, therefore, the supernatant after magnetic separation is used as the detection solution for the strip, which is the step two and shown in Scheme 1B. The strip is assembled, with AuNPs-DNA1 uniformly spread on CP, and Str-Bio-capDNA1 and Str-Bio-capDNA2 immobilized on the T zone and C zone, respectively. Since the 5′-ternimal of cDNA is designed to be complementary to DNA1 and the 3′-ternimal of cDNA complementary to capDNA1, cDNA in the detection solution can mediate the hybridization and formation of sandwich-like Str-Bio-capDNA1/cDNA/DNA1-AuNPs structure on the T zone. The captured AuNPs on the T zone makes an observable deep red band, *i.e.* a positive result on the T zone indicates the presence of kanamycin. Moreover, the accumulation of AuNPs on the T zone depends on the concentration of cDNA and therefore the concentration of kanamycin, which thus can be used for qualitive and quantitative analysis of kanamycin (Scheme 1C). Meanwhile, capDNA2 is designed to be complementary to DNA1. Thus the capture of excess DNA1-AuNPs through the formation of Str-Bio-capDNA2/DNA1-AuNPs complex on the C zone ensures that the C zone can constantly exhibit a clear deep red band. However, in the absence of kanamycin, no cDNA can be displaced from MMS-apt-cDNA in step one, thus no AuNPs can be captured on the T zone and no red band can be observed, *i.e.* the negative result on the T zone indicates the absence of kanamycin (Scheme 1D).

3.2. Synthesis and modification of AuNPs

AuNPs was synthesized by the conventional citrate reduction method and used as visible probe in the strip. The prepared AuNPs was characterized by transmission electron microscope (TEM). As shown in Fig. 1A, AuNPs are well-dispersed and with the uniform particle size around 13 nm, which is in accordance with references [28]. The absorption spectra of AuNPs were measured using a UV–vis spectrophotometer. Fig. 1B shows that a typical adsorption peak of AuNPs at 520 nm can be observed in the absorption curve.

AuNPs were then used to prepare AuNPs-DNA1 through the covalent attachment of DNA1 *via* Au–S bond. The coverage of DNA1 on the surface of AuNP will not only affect the hybridization efficiency between DNA1 and cDNA and thus the capture efficiency of AuNPs on the T zone, but also the stability and dispersibility of AuNPs on the strip. The concentration of DNA1 used to functionalize AuNPs, which is a key factor deciding the coverage of DNA1 on AuNPs, was thereby investigated and optimized. During the optimization, the stability and dispersibility of AuNPs in high concentration of NaCl was used as an indicator [31]. Different concentrations of DNA1 (0, 0.2, 0.5, 0.8, 1.0, 1.5, 2.0, 2.5, 3.0, 4.0 and 5.0 μM) was incubated with the concentrated AuNPs, then NaCl was added to maintain the final concentration of 20 mM. As shown in Fig. 1C, when DNA1 used to functionalize AuNPs is less than 4 μM, the color of AuNPs-DNA1 becomes gray upon addition of NaCl, indicating the aggregation of AuNPs. On the contrary, the color remains unchanged when DNA1 is higher than 4 μM. Therefore, the optimum concentration of DNA1 is 4 μM.

3.3. Optimization of parameters for preparation of the strip and detection

The experiment conditions during the preparation of the strip biosensor, as well as detection were systematically optimized to obtain the best performance, *i.e.* ensure the appearance of clear deep red bands on the T and C zones. The optical density of the T zone determined by colloidal gold scanning reader was used as indicator during the optimization.

The complementary sequence of cDNA to the aptamer was firstly inverstigated. Not only the length of the complementary region, but also the location of the complementary region on cDNA and the aptamer will affect the binding strength of the apt-cDNA duplex. An appropriate complementary sequence can maintain the stability of the duplex, whereas makes cDNA easily be competitively displaced by kanamycin. Thus different sequences of cDNA that are complementary to the different region of the aptamer were designed (Fig. 2A) and used to prepare MMS-apt-cDNA conjugate. 5 mM kanamycin was used as sample, which was pretreated with respective MMS-apt-cDNA conjugates and tested with the strip. The optical density of the T zone was then determined. It can be seen in Fig. 2A that sufficiently higher optical density of the band appears on the T zone when cDNA sequence 6 is employed. Therefore, sequence 6 was chosen as the optimal sequence of cDNA.

In step 1, the samples containing kanamycin is firsty pretreated with MMS-apt-cDNA to convert kanamycin to the released cDNA. The amount of magnetic microspheres used will decide the total load of apt-cDNA on magnetic microspheres, which can be displaced by kanamycin. Therefore the amount of magnetic microspheres was optimized. Different amounts of magnetic microspheres ranging from 0.1 to 1.0 mg/mL were used to combine with apt-cDNA to prepare MMS-apt-cDNA, and then pretreat and detect 5 mM kanamycin. The result is shown in Fig. 2B. The peak area of the T zone gradually increases with the increase of the amount of magnetic microspheres and then remains constant when the amount reaches 0.75 mg/mL. Thus, the optimum amount of magnetic microspheres was determined to be 0.75 mg/mL.

During the pretreatment, it is important to ensure the complete displacement of cDNA from MMS-apt-cDNA complex by kanamycin. Then the reaction conditions including incubation time, temperature and oscillation rate were optimized. Keeping the other reaction conditions constant, the incubation time of kanamycin and MMS-apt-cDNA was optimized. As shown in Fig. 2C, with the increase of the incubation time, the peak area of the T zone increases. When the incubation time is longer than 10 min, the peak area is basically stable. In order to save the detection time, 10 min is the most suitable incubation time. The incubation temperature was then also optimized, which was set as 20 °C, 25 °C, 30 °C, 37 °C and 45 °C, respectively. As shown in Fig. 2D, the peak area almost keeps constant when the temperature is higher than 25 °C. Then the typical room temperature of 25 °C was chosen for incubation, which makes the strip biosensor more practical. The characteristic of easy to precipitate of magnetic microspheres affects the competitively binding of kanamycin to aptamer. So oscillation is required during the incubation. The shock speed was set to be 0, 50, 100, 150, 200 and 220 rpm, respectively, and the results are shown in Fig. 2E. The peak area of the T zone is basically the same at different oscillation rate (except for the oscillation rate of 0). This proves that a slight shock can prevent magnetic microspheres from settling down. In summary, during the pretreatment, kanamycin samples are incubated with MMS-apt-cDNA at room temperature for 10 min with mild oscillation.

The biotinylated capDNA1 and capDNA2, which are fixed on the T zone and the C zone through streptavidin, need to be pre-bound with streptavidin to form Str-Bio-capDNA1 and Str-Bio-capDNA2, respectively. Then the concentration of streptavidin was optimized. The same concentration of capDNA1 and capDNA2 were incubated with different concentrations of streptavidin for 2 h and fixed on NC membrane. As shown in Fig. 2F, the peak areas of the T and C zones increase with the increase of the concentration of streptavidin, and reach saturated when the concentration reaches 0.5 mg/mL. Thus 0.5 mg/mL streptavidin was used to prepare Str-Bio-capDNAs.

Finally, the concentrations of Str-Bio-capDNA1 and Str-Bio-capDNA2, which influence the accumulation of AuNPs on the T and C zones and the color depth of the bands were optimized. Different concentrations of Str-Bio-capDNA1 and Str-Bio-capDNA2 (refer to the concentration of capDNA1 and capDNA2) were employed to prepare the T and C zones, and the test strips were assembled and tested. As shown in Fig. 2G, with the increase of capDNA1, the peak area of the T zone gradually increases. When the concentration reaches 7.5 μM, the peak area remains constant. Meanwhile, with the increase of capDNA2, the peak area of the C zone gradually increases, until the concentration reaches 2.5 μM. Therefore, the optimum concentrations of Str-Bio-capDNA1 and Str-Bio-capDNA2 were determined to be 7.5 μM and 2.5 μM.

3.4. Evaluation of the performance of the strip biosensor

The strip biosensor was fabricated and used under the above optimal conditions. Kanamycin samples were qualitatively detected by naked eyes or quantitatively detected by using a scanning reader.

Kanamycin standard solution within the concentration range of 0–5 mM was firstly pretreated with MMS-apt-cDNA complex. And the supernatant containing released cDNA was used as detection solution for the strip biosensor because the concentration of cDNA is proportional to that of kanamycin. The results are shown in Fig. 3A. Str-Bio-capDNA1 on the T zone cannot capture AuNPs without kanamycin because cDNA which mediates the formation of sandwich-like Str-Bio-capDNA1/cDNA/DNA1-AuNPs structure is not produced in the absence of kanamycin. However, the capture of AuNPs on the C zone by Str-Bio-capDNA2 does not need cDNA. Thus only one red band displayed on the C zone in the absence or in the presence of very low concentration of kanamycin. With the increase of kanamycin concentration, the color of the C zone is basically unchanged, whereas the color of the T zone is gradually deepened, owing to the accumulation of AuNPs on the T zone. When the concentration of kanamycin reaches 50 nM, a slight red band can be observed on the T zone by naked eyes. Therefore, 50 nM is the visual detection limit of the strip biosensor. The peak areas of the T

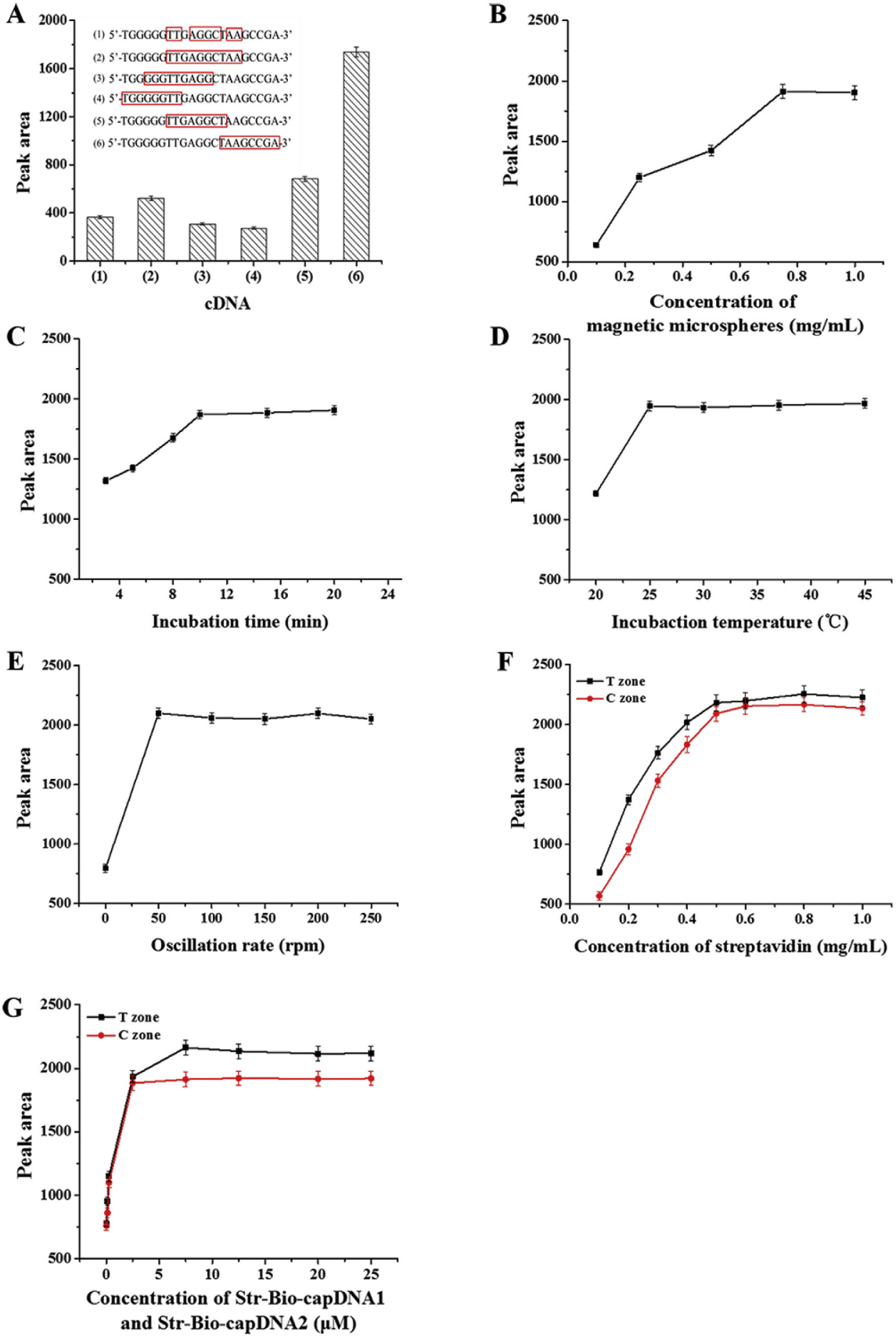

Fig. 2. Optimization of parameters (n = 3): (A) sequence of cDNA and its complementary region to the aptamer; Inset shows the sequence and the complementary region; (B) amount of magnetic microspheres; (C) incubation time; (D) incubation temperature; (E) oscillation rate; (F) concentration of streptavidin; (G) concentration of Str-Bio-capDNA1 and Str-Bio-capDNA2.

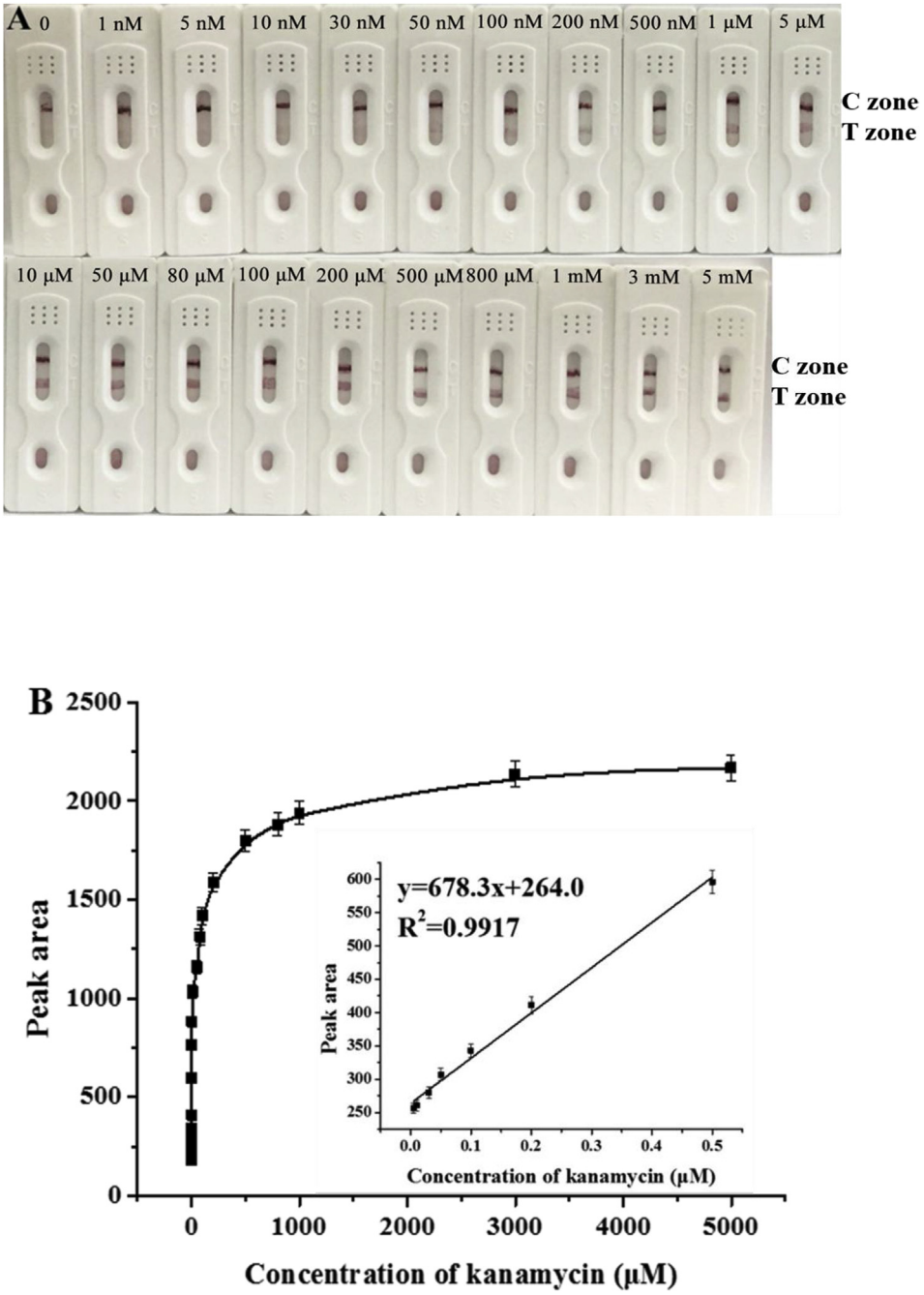

Fig. 3. (A) The photograph of the strips applied with different concentrations of kanamycin; (B) The relationship between the peak area of the T zone and the concentration of kanamycin in standard solution; Inset shows the linear relationship (n = 3).

Table 1
Comparison of the aptamer-based strip with other reported methods.

Method	Detection limit	Linear range	Sample	Reference
Electrochemical detection	0.06 nM	0.1–60 nM	Honey	[14]
HPLC	65.23 μM	/	Pharmaceutical analysis	[10]
Indirect competitive ELISA	0.02 nM	0.09–545 nM	Pork, chicken, milk	[13]
SPR	1.0 ± 0.10 pM	/	Milk	[12]
CZE	12.02 nM	36.05 nM-85.83 μM	Milk	[11]
Colorimetric detection	0.68 μM	1–40 μM	Milk	[32]
Fluorescence resonance energy transfer assay	13.52 nM	100–600 nM	Milk	[33]
Colloidal gold lateral flow strip biosensor	4.96 nM	5–500 nM	Milk, honey, milk powder	This study

Table 2
The comparison of the strip assay with HPLC.

Concentration of kanamycin added (mM)	Strip biosensor (n = 3)		HPLC (n = 3)	
	Average (mM)	RSD (%)	Average (mM)	RSD (%)
3	2.94	4.96	2.95	0.59
10	10.52	4.26	10.05	0.25
15	14.77	2.15	15.03	0.32

zones of different test strips were measured and plotted to the concentration of kanamycin, as shown in Fig. 3B. The peak area gradually increases with the increase of kanamycin concentration. The inset of Fig. 3B shows a linear response of the peak area to the concentration of kanamycin over a wide nanomolar range (5–500 nM). The linear regression equation is $y = 678.3x + 264.0$ ($R^2 = 0.9917$), where x is the concentration of kanamycin (nM), and y is the peak area. The detection limit of 4.96 nM can be derived (S/N = 3). The performance of the developed strip biosensor was compared with other reported methods (Table 1). Although the detection limit of this work is not the lowest, it offers very short detection time and can be used for on-site determination. Meanwhile, the detection limit of the strip biosensor is far lower than the MRLs for kanamycin in food stuffs, which can meet the reqirement of food analysis. Since HPLC is a common method for antibiotics detection, the accuracy of the strip biosensor fabricated in this paper was verified by comparison the results with those of HPLC analysis. The two methods were both performed to detect standard kanamycin samples with the concentration of 3, 10 and 15 mM, respectively, and the results are shown in Table 2. The results from both methods are similar and accurate. In term of RSD value, the strip biosensor is higher than HPLC. But with the value lower than 5%, it is also sufficient to meet application requirements.

To assess the selectivity of the strip biosensor for kanamycin, various other antibiotics including streptomycin (STR), ampicillin (AMP), neomycin (NEO), gentamicin (GEN), as well as kanamycin and water were applied to the strip biosensor. The concentration of the antibiotics was fixed to 5 mM. The optical densities of the T zones were then determined and compared. As shown in Fig. 4, compared with the negative control (water), only kanamycin exhibits a significant increased peak area of the T zone, indicating the high specificity of the strip to kanamycin.

To evaluate the stability of the strip biosensor, the prepared strips and MMS-apt-cDNA were both stored at 4 °C under dry condition for different peroid (0, 3, 7, 15, 30, 60 and 90 days), and then used to detect different concentrations of kanamycin (0, 30 nM, 100 nM, 10 μM, 100 μM and 500 μM). As shown in Fig. 5, the peak areas of the T zones on the strips for different concentrations of kanamycin are merely

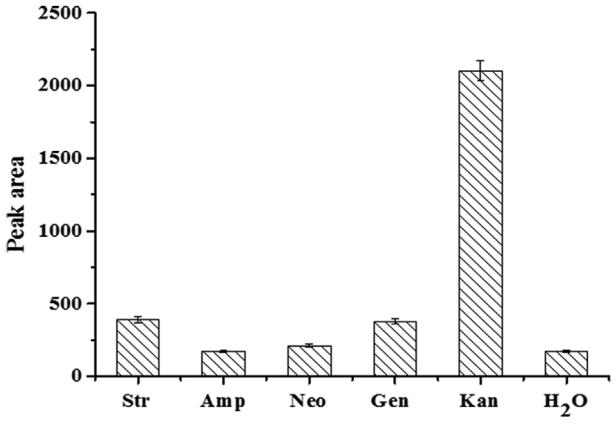

Fig. 4. Specificity evaluation of the strip biosensor (n = 3).

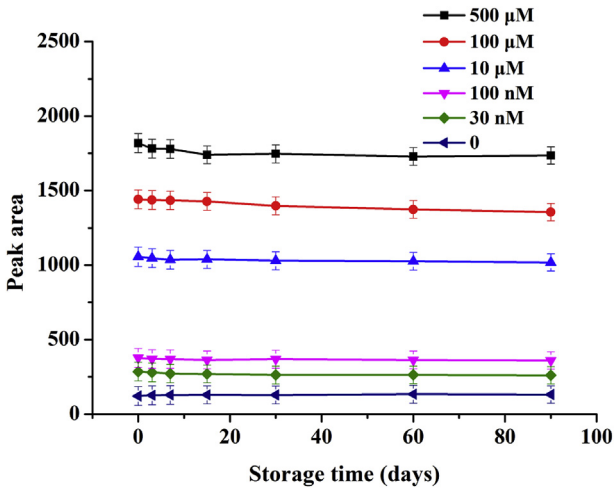

Fig. 5. Storage stability of the strip biosensor (n = 3).

changed (only 3.60%–9.84% faded) after 3 months storage, indicating satisfactory stability of the strip biosensor.

3.5. Evaluation of the practicability of the strip biosensor

Artificially contaminated food samples, including milk, honey and milk powder, were prepared and used to evaluate the practicability of the strip biosensor. Different concentrations of kanamycin (0, 30 nM, 50 nM, 100 nM, 200 nM, 500 nM, 1 μM, 10 μM and 100 μM) were spiked into kanamycin-free food samples. Pretreatment is required for milk and milk powder samples to remove fat and proteins. For honey samples, simple dilution is effective. Then these real samples were pretreated with MMS-apt-cDNA and tested by the strips, which were just the same with those of standard samples. The results are shown in Fig. 6. The visual detection limits for kanamycin in milk, honey and milk powder samples are 50 nM (29.13 ng/g), 50 nM (29.13 ng/g) and 100 nM (58.26 ng/g), respectively. The visual detection limits for milk and honey samples are basically consistent with the standard solution. For milk powder samples, the detection limit is slightly higher, but within the acceptable range. Therefore, the strip biosensor has great application prospects in detection of kanamycin in actual food samples.

4. Conclusion

To sum up, we have successfully developed a colloidal gold lateral flow strip biosensor for kanamycin. Employing magnetic microspheres-based fast separation and functionalized AuNPs-based coloration, rapid detection of kanamycin can be achieved within 20 min for the two-step procedure. The strip exhibits excellent sensitivity, specificity and stability. Compared to the traditional aptamer-based lateral strip biosensors, which rely on the quantification of the concentration of the aptamers, this strip relies on the concentration of cDNA. This not only offers more intuitive and sensitive result, but also broadens the application of the strips through the customization of the sequence and length of cDNA. The verification of the practicability of the strip biosensor by challenging multiple kanamycin-spiked food samples suggests the prospects of the strip biosensor for rapid, simple, low-cost and on-site detection of kanamycin in diverse areas.

Conflicts of interest

None.

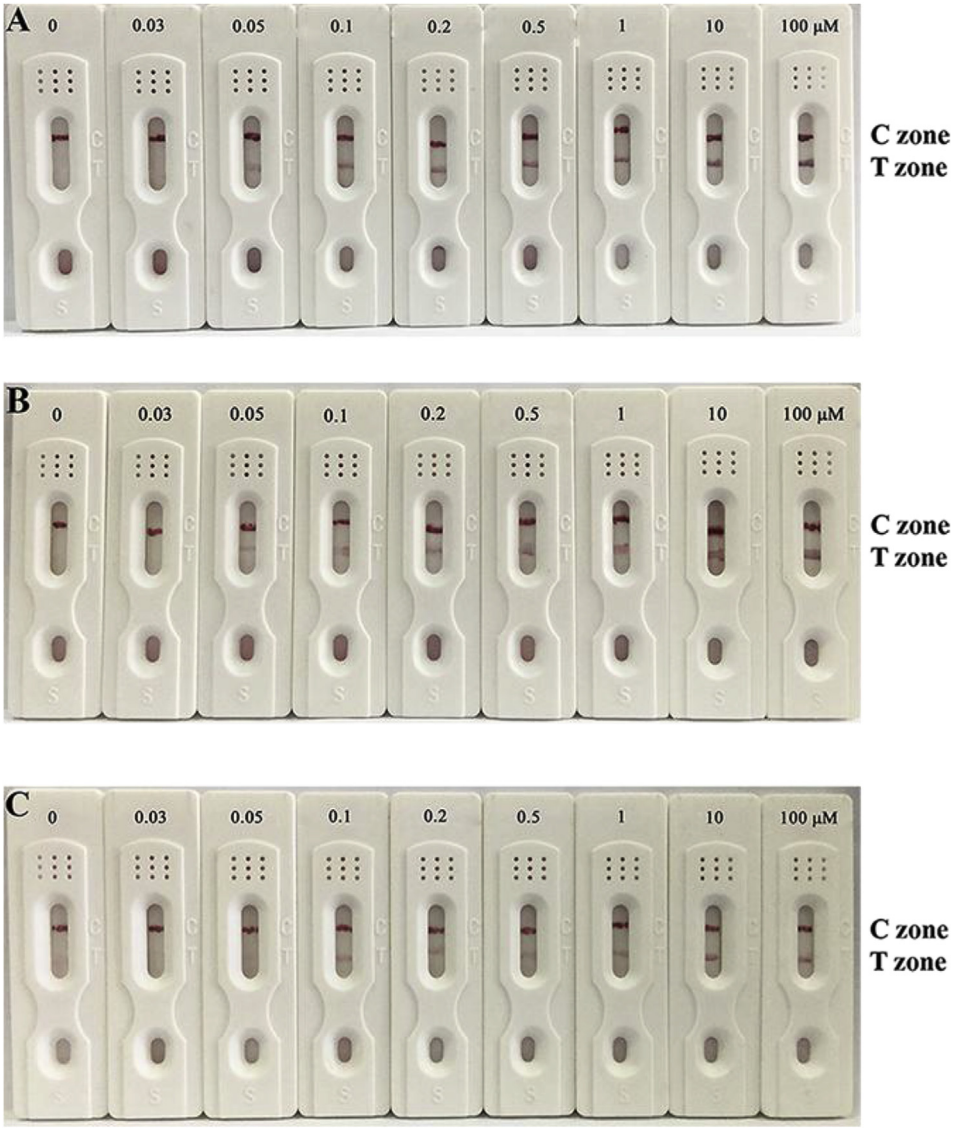

Fig. 6. Detection of kanamycin in real samples: (A) milk samples; (B) honey samples; (C) milk powder samples.

Acknowledgements

This work was supported by the National Natural Science Foundation of China (no. 31271860) and the Six Talent Peaks Project in Jiangsu Province (JY-078).

References

[1] C. Li, Y. Zhang, S.A. Eremin, O. Yakup, G. Yao, X. Zhang, Detection of kanamycin and gentamicin residues in animal-derived food using IgY antibody based ic-ELISA and FPIA, Food Chem. 227 (2017) 48–54 https://doi.org/10.1016/j.foodchem.2017.01.058.

[2] J. Chen, Z. Li, J. Ge, R. Yang, L. Zhang, L.B. Qu, H.Q. Wang, L. Zhang, An aptamer-based signal-on bio-assay for sensitive and selective detection of kanamycin A by using gold nanoparticles, Talanta 139 (2015) 226–232 https://doi.org/10.1016/j.talanta.2015.02.036.

[3] L.S. Khabbaz, M. Hassanzadeh-Khayyat, P. Zaree, M. Ramezani, K. Abnous, S.M. Taghdisi, Detection of kanamycin by using an aptamer-based biosensor using silica nanoparticles, Anal. Methods 7 (2015) 8611–8616 https://doi.org/10.1039/c5ay01807b.

[4] N.C. Megoulas, M.A. Koupparis, Direct determination of kanamycin in raw materials, veterinary formulation and culture media using a novel liquid chromatograph - evaporative light scattering method, Anal. Chim. Acta 547 (2005) 64–72 https://doi.org/10.1016/j.aca.2004.11.031.

[5] R.Y. Robati, A. Arab, M. Ramezani, F.A. Langroodi, K. Abnous, S.M. Taghdisi, Aptasensors for quantitative detection of kanamycin, Biosens. Bioelectron. 82 (2016) 162–172 https://doi.org/10.1016/j.bios.2016.04.011.

[6] H.Y. Song, T.F. Kang, N.N. Li, L.P. Lu, S.Y. Cheng, Highly sensitive voltammetric determination of kanamycin based on aptamer sensor for signal amplification, Anal. Methods 8 (2016) 3366–3372 https://doi.org/10.1039/c6ay00152a.

[7] Y.P. Xing, C. Liu, X.H. Zhou, H.C. Shi, Label-free detection of kanamycin based on a G-quadruplex DNA aptamer-based fluorescent intercalator displacement assay, Sci. Rep. 5 (2015), https://doi.org/10.1038/srep08125.

[8] S. Yan, X. Lai, Y. Wang, N. Ye, Y. Xiang, Label free aptasensor for ultrasensitive detection of tobramycin residue in pasteurized cow's milk based on resonance scattering spectra and nanogold catalytic amplification, Food Chem. 295 (2019) 36–41 https://doi.org/10.1016/j.foodchem.2019.05.110.

[9] European Commission, Commission Regulation (EU) No. 37/2010 of 22 December 2009: on Pharmacologically Active Substances and Their Classification Regarding Maximum Residue Limits in Foodstuffs of Animal Origin, J. Eur. Union, 2010, pp. 1–72.

[10] B. Blanchaert, E. Poderós Jorge, P. Jankovics, E. Adams, A. Van Schepdael, Assay of kanamycin A by HPLC with direct UV detection, Chromatographia 76 (2013) 1505–1512 https://doi.org/10.1007/s10337-013-2440-8.

[11] C.Z. Yu, Y.Z. He, G.N. Fu, H.Y. Xie, W.E. Gan, Determination of kanamycin A, amikacin and tobramycin residues in milk by capillary zone electrophoresis with post-column derivatization and laser-induced fluorescence detection, J. Chromatogr. B: Anal. Technol. Biomed. Life Sci. 877 (2009) 333–338 https://doi.org/10.1016/j.jchromb.2008.12.011.

[12] M. Frasconi, R. Tel-Vered, M. Riskin, I. Willner, Surface plasmon resonance analysis of antibiotics using imprinted boronic acid-functionalized Au nanoparticle composites, Anal. Chem. 82 (2010) 2512–2519 https://doi.org/10.1021/ac902944k.

[13] J. He, Y. Wang, X. Zhang, Preparation of artificial antigen and development of IgY-based indirect competitive ELISA for the detection of kanamycin residues, Food Anal. Methods 9 (2016) 744–751 https://doi.org/10.1007/s12161-015-0248-x.

[14] C. Wang, C. Liu, J. Luo, Y. Tian, N. Zhou, Direct electrochemical detection of

kanamycin based on peroxidase-like activity of gold nanoparticles, Anal. Chim. Acta 936 (2016) 75–82 https://doi.org/10.1016/j.aca.2016.07.013.
[15] W. Guo, N. Sun, X. Qin, M. Pei, L. Wang, A novel electrochemical aptasensor for ultrasensitive detection of kanamycin based on MWCNTs-HMIMPF6 and nanoporous PtTi alloy, Biosens. Bioelectron. 74 (2015) 691–697 https://doi.org/10.1016/j.bios.2015.06.081.
[16] Y. Zhu, P. Chandra, K.M. Song, C. Ban, Y.B. Shim, Label-free detection of kanamycin based on the aptamer-functionalized conducting polymer/gold nanocomposite, Biosens. Bioelectron. 36 (2012) 29–34 https://doi.org/10.1016/j.bios.2012.03.034.
[17] H. Wang, Y. Wang, S. Liu, J. Yu, Y. Guo, Y. Xu, J. Huang, Signal-on electrochemical detection of antibiotics at zeptomole level based on target-aptamer binding triggered multiple recycling amplification, Biosens. Bioelectron. 80 (2016) 471–476 https://doi.org/10.1016/j.bios.2016.02.014.
[18] W. Liu, M. Zhang, X. Liu, A. Sharma, X. Ding, A Point-of-Need infrared mediated PCR platform with compatible lateral flow strip for HPV detection, Biosens. Bioelectron. 96 (2017) 213–219 https://doi.org/10.1016/j.bios.2017.04.047.
[19] Q. Zhang, Q. Qu, S. Chen, X. Liu, P. Li, A double-label time-resolved fluorescent strip for rapidly quantitative detection of carbofuran residues in agro-products, Food Chem. 231 (2017) 295–300 https://doi.org/10.1016/j.foodchem.2017.02.016.
[20] Z.P. Liang, W.Z. Ha, Z.L. Xiao, H.T. Lei, Y.D. Shen, Y.M. Sun, H. Wang, J.Y. Yang, Z.L. Xu, Development of a simple, fast, and quantitative lateral flow immunochromatographic strip for folic acid, Food Anal. Methods 10 (2017) 2444–2453 https://doi.org/10.1007/s12161-017-0804-7.
[21] A. Chen, S. Yang, Replacing antibodies with aptamers in lateral flow immunoassay, Biosens. Bioelectron. 71 (2015) 230–242 https://doi.org/10.1016/j.bios.2015.04.041.
[22] Y.S. Kim, N.H. Raston, M.B. Gu, Aptamer-based nanobiosensors, Biosens. Bioelectron. 76 (2016) 2–19 https://doi.org/10.1016/j.bios.2015.06.040.
[23] S.Y. Toh, M. Citartan, S.C. Gopinath, T.H. Tang, Aptamers as a replacement for antibodies in enzyme-linked immunosorbent assay, Biosens. Bioelectron. 64 (2015) 392–403 https://doi.org/10.1016/j.bios.2014.09.026.
[24] S. Wu, L. Liu, N. Duan, Q. Li, Y. Zhou, Z. Wang, Aptamer-based lateral flow test strip for rapid detection of zearalenone in corn samples, J. Agric. Food Chem. 66 (2018) 1949–1954 https://doi.org/10.1021/acs.jafc.7b05326.
[25] K.M. Song, M. Cho, H. Jo, K. Min, S.H. Jeon, T. Kim, M.S. Han, J.K. Ku, C. Ban, Gold nanoparticle-based colorimetric detection of kanamycin using a DNA aptamer, Anal. Biochem. 415 (2011) 175–181 https://doi.org/10.1016/j.ab.2011.04.007.
[26] X. Han, Y. Zhang, J. Nie, S. Zhao, Y. Tian, N. Zhou, Gold nanoparticle based photometric determination of tobramycin by using new specific DNA aptamers, Microchim. Acta 185 (2018), https://doi.org/10.1007/s00604-017-2568-6.
[27] J. Nie, L. Yuan, K. Jin, X. Han, Y. Tian, N. Zhou, Electrochemical detection of tobramycin based on enzymes-assisted dual signal amplification by using a novel truncated aptamer with high affinity, Biosens. Bioelectron. 122 (2018) 254–262 https://doi.org/10.1016/j.bios.2018.09.072.
[28] J. Liu, J. Zeng, Y. Tian, N. Zhou, An aptamer and functionalized nanoparticle-based strip biosensor for on-site detection of kanamycin in food samples, Analyst 143 (2018) 182–189 https://doi.org/10.1039/c7an01476g.
[29] X. Gao, L.P. Xu, T. Wu, Y. Wen, X. Ma, X. Zhang, An enzyme-amplified lateral flow strip biosensor for visual detection of microRNA-224, Talanta 146 (2016) 648–654 https://doi.org/10.1016/j.talanta.2015.06.060.
[30] W. Zhou, W. Kong, X. Dou, M. Zhao, Z. Ouyang, M. Yang, An aptamer based lateral flow strip for on-site rapid detection of ochratoxin A in *Astragalus membranaceus*, J. Chromatogr. B: Anal. Technol. Biomed. Life Sci. 1022 (2016) 102–108 https://doi.org/10.1016/j.jchromb.2016.04.016.
[31] C. Qin, W. Wen, X. Zhang, H. Gu, S. Wang, Visual detection of thrombin using a strip biosensor through aptamer-cleavage reaction with enzyme catalytic amplification, Analyst 140 (2015) 7710–7717 https://doi.org/10.1039/c5an01712b.
[32] C. Xu, Y. Ying, J. Ping, Colorimetric aggregation assay for kanamycin using gold nanoparticles modified with hairpin DNA probes and hybridization chain reaction-assisted amplification, Microchim. Acta 186 (2019), https://doi.org/10.1007/s00604-019-3574-7.
[33] X. Ma, S. Qiao, H. Sun, R. Su, C. Sun, M. Zhang, Development of structure-switching aptamers for kanamycin detection based on fluorescence resonance energy transfer, Front. Chem. 7 (2019), https://doi.org/10.3389/fchem.2019.00029.